DEVELOPMENT OF TRACTIVE PERFORMANCE PREDICTION FOR FLEXIABLE WHEEL

Yalda Favaedi[(1)], Alexandre Pechev[(1)]

[(1)]Surrey Space Centre, University of Surrey, Guildford, GU2 7XH, U.K.
y.favaedi@surrey.ac.uk, a.pechev@surrey.ac.uk

ABSTRACT:

Planetary rovers are typically developed for high-risk missions to operate in difficult terrains, including slopes, terrains with obstacles and on soft and hard soils. In soft soils, traction is limited by the mechanical properties of the soil therefore lack of traction and wheel slippage cause difficulties during the operation of the rover. Operating the vehicle on a soft ground is different than operating it on a prepared firm road. Locomotion requires traction to provide forward thrust on the ground. Traction force is the main force in the terrain, not only available to accelerate the vehicle but also to climb up slopes or to run over obstacles. One possibility to raise the traction is to increase the wheel-ground contact area size. Flexible wheels provide this as they increase the contact length due to the wheel's deformation under load and hence decrease ground pressure on soil surface. Rigid wheels have been extensively studied in the past and important theories have been established and validated through simulations and experiments. Little, however, has been done on developing theory for flexible wheels for quantifying the performance. In this study the Bekker theory has been extended by developing analytical models that predict the tractive performance for a flexible metal wheel by using the geometric model of the wheel in deformation.

Nomenclature

A	Contact patch in section BC $[m^2]$	θ_{df}	Deformation angle $[Rad]$
a	Semi major axis of ellipse	P_2	Average ground pressure $[Pa]$
b	Semi minor axis of ellipse	w	Wheel load $[N]$
B	Wheel width $[m]$	ϕ	Internal Friction angle $[°]$
c	Soil cohesion $[Pa]$	w_1	wheel load in section CD $[N]$
df_y	Wheel vertical deformation $[m]$	w_2	wheel load in section BC $[N]$
dN	Soil reaction pressure	$Z(s)$	slippage sinkage $[m]$
j_{CD}	Soil shear displacement $[m]$	h_b	height of grouse $[m]$
k	Shear deformation slip modulus $[m]$	s	slippage $[\%]$
K	Soil deformation modulus due to sinkage $[N/m^{n+2}]$	Z_0	Maximum Sinkage $[m]$
		n	Soil deformation coefficient $n[-]$
k_c	Cohesive modulus $[N/m^{n+1}]$	p_{gr}	Pressure due to wheel stiffness $[Pa]$
k_ϕ	Friction modulus $[N/m^{n+2}]$	P	Normal pressure $[Pa]$
L	Radius of the ellipse at angle θ $[m]$	θ_1	first contact angle $[Rad]$
L_1	Radius of the ellipse at angle θ_1 $[m]$	θ_2	exiting angle $[Rad]$
L_{C1}	Contact length in section BC $[m]$	$H_1(s)$	Soil thrust in Section CD $[N]$
L_{C2}	Contact length in section BC $[m]$	$H_2(s)$	Soil thrust in Section BC $[N]$
M	Arbitrary point	$\tau_1(\theta)$	Soil shear strength in section CD $[Pa]$
DP	Drawbar Pull $[N]$	σ_2	Normal Pressure in section BC $[Pa]$
$\sigma_1(\theta)$	Normal Pressure in section DC $[Pa]$		

1. INTRODUCTION

The tractive force, produced from the interaction between the wheel and the ground, determines the rover's ability to accelerate, climb slopes and cross over obstacles. Due to sinkage, rovers operating on soft soils must handle much higher resistance. Therefore reducing the sinkage is the major part of achieving an optimal tractive performance. The latter can be attained by increasing the diameter or the wheel ([1]), although this approach is restricted due to constraints such as vehicle dimensions and the power consumption. Increasing the length of the contact patch without rising the dimensions of the wheel is another approach that can be used to improve on the tractive performance. Flexible wheels including pneumatic tyre [2] and flexible metal wheels are such alternatives that provide a larger contact patch. Risk of employing pneumatic tyre, however, is considered very high in robotic missions. The flexible metal wheels thus is the only alternative that provides an increase in the length of the contact patch due to the wheel's deformation under load and a decrease in the ground pressure on the soil surface. In turn, sinkage and compaction resistance are reduced and the traction force is increased. For wheeled rough terrain rovers, the motion optimisation is somewhat related to minimizing slip. Minimizing wheel slip not only limits odometric error but also increases the robot's climbing performance. A key parameter in the minimization of slip is the contact angles between the wheel and the ground. By knowing the first contact angle through the deformation of the wheel, the slippage can be controlled by reducing the velocity of that wheel. Contact angles between the rover wheels and terrain are a key variable for traction algorithms [3, 4, 5]. However physical measurement of these angles is difficult in practice. Researchers have suggested installing costly and complex multi-axis force sensors for this [3].

In this paper, analytical models that predict the tractive performance for a flexible metal wheel are presented.
Under a typical deformation, most generally, three different contact areas between the wheel and the soil can be identified. These have been validated through numerical simulations and practical data. The key contribution of the proposed in this study method is obtaining analytically the wheel ground contact angles (for two of the contact areas) and the wheel-ground contact length (for one of the areas) based on the ground pressure for a generic flexible wheel. Subsequently, soil sinkage, motion resistance, drawbar pull and the overall performance of the wheel can be analysed from the proposed new analytical model for flexible wheels. The developments have been validated by Finite Elements numerical models to show a close comparison with the analytical results. Simulation results presented in this paper illustrate that the flexible wheel increases the traction force and hence better slippage control can be achieved in comparison to a rigid wheel with the same dimensions

2. WHEEL PHYSICAL MODEL

The flexible wheel considered in this study was taken from the design proposed by Deutsche Zentrum Fur Luft-und Raumfahrt (DLR) [6]. The baseline of design is an all-metallic configuration with 3 rows of leaf springs mounted to a rigid hub. A rigid "bump stop" prevents excessive deflection of the spring elements. The design concept is closely based one the "MOVE2 ocean floor vehicle developed by the University of Bremen and DLR. Wheel diameter and width are 30 cm and 10 cm respectively and load distribution on each wheel is 50 kg.

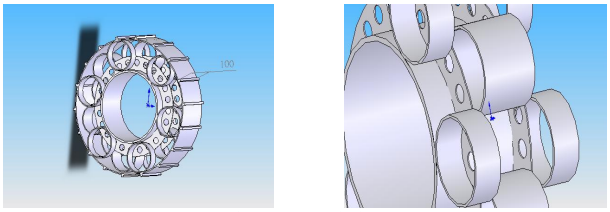

Fig. 1. Flexible wheel

3. DEVELOPMENT OF FLEXIBLE WHEEL-SOIL INTERACTION MODEL

3.1. Ground Pressure Distribution:

When a flexible wheel is running upon a terrain, if the average ground pressure of the wheel p_{gr} (the pressure produced by the stiffness of the wheel) is greater than the maximum pressure that terrain can support at the lowest point

of the wheel circumference, the wheel remains round like a rigid wheel. Other wise the wheel acts as a flexible wheel and thus it will change its shape to an ellipse in the lower section of the wheel rim.
For our modelling and investigation the portion of the circumference of the wheel which is in contact with the soil is divided into three sections as shown in "Fig.2" forward part CD, middle part BC, and rear part AB.
Along section CD, the shear displacement rises, and the normal pressure and the shear stress both increase. On the flat section BC, the normal pressure remains constant and equal to the average ground pressure; however, the shear stress increases with the shear displacement. Along the section AB, both the normal pressure and the shear stress decrease while the shear displacement increases slightly. However this section is assumed to be a negligible quantity (i.e. $\theta_2 \approx 0$).

For the section CD $\theta_{df} \le \theta \le \theta_1$, the maximum amount of sinkage and the sinkage at any arbitrary angle are derived by "(1)" "(2) respectively.

$$Z_0 = b - df_y - L_1 \cos\theta_1 \tag{1}$$

$$Z = L\cos\theta - L_1 \cos\theta_1 \tag{2}$$

Applying the Bekker's equation for the pressure-sinkage relation, shown in (3), the normal pressure increases along section CD.

$$\sigma(\theta) = -P(\theta) = -KZ^n \tag{3}$$

$$\sigma_1(\theta) = -\left(\frac{k_c}{B} + k_\phi\right).\left(L\cos\theta - L_1\cos\theta_1\right)^n \tag{4}$$

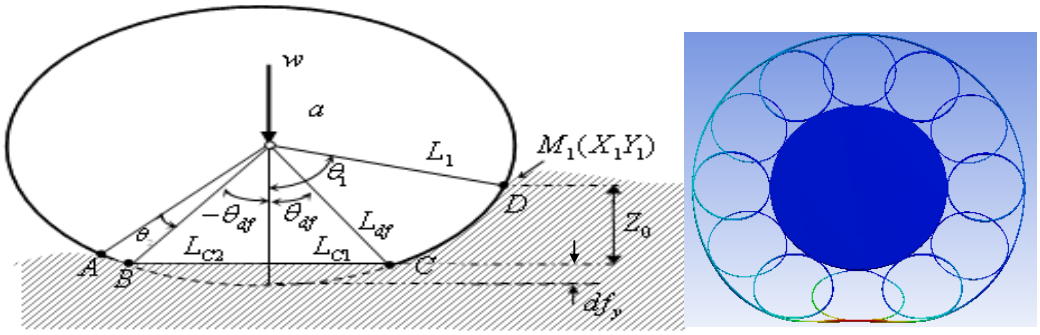

Fig. 2. Wheel Deformation

For the flat section BC $\theta_{-df} \le \theta \le \theta_{df}$ the normal pressure is uniform and equals to the average ground contact pressure P_{gr}.

$$\sigma_2 = -K\left(b - df_y - L_1\cos\theta_1\right)^n \tag{5}$$

3.2. The first Contact angle for flexible wheel:

The distribution of the ground reaction applies to the peripheral surface of the flexible wheel during rest position. The soil reaction *N* is the sum of the simple reaction dN of the ground resistance against rolling [1]. The reactions are presumed to be perpendicular to the circumference of the wheel therefore according to "Fig.3"; the following equations can be derived:

$$w = \int_{-\theta_{df}}^{\theta_1} dN \cos\theta \tag{6}$$
$$dN\cos\theta = pBds\cos\theta$$

ds is the arc length from $\theta = \theta_1$ to $\theta = -\theta_{df}$ and can be expressed as:

$$X = L\sin\theta$$
$$Y = L\cos\theta$$
$$\frac{dX}{d\theta} = L\cos\theta$$
$$\frac{dY}{d\theta} = -L\sin\theta$$

$$ds = Ld\theta \tag{7}$$

The wheel axel load can be determined by combining (1), (2), (3) (6), and (7). The load is divided between the contact pressure distribution in section BC and CD.

$$w = w_1 + w_2 \tag{8}$$

$$\begin{aligned} w &= BK\int_{\theta_{df}}^{\theta_1} L\left(L\cos\theta + L_1\cos\theta_1\right)^n \cos\theta d\theta \\ &+ BK\int_{-\theta_{df}}^{\theta_{df}} L\left(b - df_y - L_1\cos\theta_1\right)^n \cos\theta d\theta \end{aligned} \tag{9}$$

The fist contact angle can be determined by the load equation above by identifying a numerical solution.
As shown in "Fig.2" and "Fig.3", the radial distribution of soil reaction to the flexible wheel circumference during driving situation can be expressed by the wheel normal stress and shear strength around the contact parts.

$$\begin{aligned} w &= B\int_{\theta_{df}}^{\theta_1} \left(L\left(\sigma_1(\theta)\cos\theta + \tau_1(\theta)\sin\theta\right)\right)d\theta \\ &+ B\int_{-\theta_{df}}^{\theta_{df}} L\sigma_2\cos\theta d\theta \end{aligned} \tag{10}$$

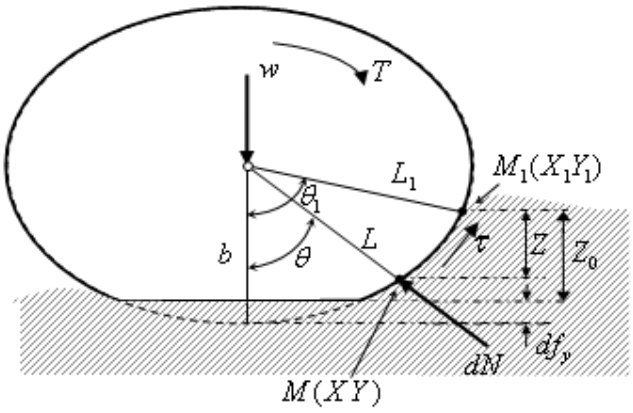

Fig. 3. Determination of the first contact angle

Equation (10) employs to predict the first contact angle of a driven flexible wheel .The vertical component of shear stress at the contact area of the section CD can be neglected to simplify the flexible wheel –soil interaction model. Subsequently, soil sinkage, motion resistance, drawbar pull and the overall performance of the flexible wheel can be calculated.

3.3. Soil thrust and Drawbar pull

Locomotion requires traction to provide forward thrust on the ground [1, 7]. The maximum force that can be continued by the soil before extreme slippage occurs is known as soil thrust [8].

Shear strength depends on the contact angle between wheel and soil at section CD and can be described by (11) [1,8].

$$\tau_1(\theta) = \left[c + \sigma_1(\theta)\tan\phi\right]\left(1 - e^{\frac{-J_{CD}}{k}}\right) \tag{11}$$

The soil trust for flexible wheel along section CD can be calculated by using (7) and (11).

$$H_1(s) = B\int_{\theta_{df}}^{\theta_1} L\tau_1(\theta)\cos\theta.d\theta \tag{12}$$

The soil thrust in section BC is determined by the shear strength of the terrain and the contact area due to uniform pressure distribution thus soil thrust in this section is not increasing by θ can be derived by (13)[8].

$$H_2(s) = A.c + w_2.\tan\phi\left(1 - \frac{k}{s.L_C}\left(1 - e^{\frac{-s.L_C}{K}}\right)\right) \tag{13}$$

$$L_C = 2.L_{C1} = 2.\left(b - df_y\right).\tan\left(\theta_{df}\right)$$

The soil trust for a whole flexible wheel can be finally calculated

$$H(s) = H_1(s) + H_2(s)$$

Drawbar pull (DP) is the difference between soil thrust H and motion resistance R [1, 7].

$$DP = H - R$$

$$R = R_c + R_b + R_r$$

Bulldozing resistance (R_b) is much less than compaction resistance (R_c). Also, rolling resistance is likely to be a minor factor to overall resistance [1].
The compaction resistance for a flexible wheel is:

$$R_c(s) = B.K\frac{Z_t(s)^{n+1}}{n+1} \tag{14}$$

$$h = 1.2h_b$$

$$Z(s) = 2hs$$

$$Z_t(s) = Z_0 + Z(s)$$

$$DP(s) = H(s) - R_c(s) \tag{15}$$

4. RESULTS:

In this section we investigate the proposed in this paper models for estimating DP. We use finite element analyses to measure the deformation of the flexible wheel (df_y); in a practical scenario this information is provided by sensor mounted on the wheel. This model includes a flexible wheel which runs on a 3-dimensional terrain profile. To analyze the proposed models, several scenarios have been simulated. "Fig .4" illustrates the draw bar pull and compaction resistance versus slippage for a flexible wheel and a rigid wheel as derived by our models. In this analysis, it is assumed that both wheels move on a low depth sandy surface. As indicated in the results, the flexible wheel shows better performance even for a small vertical deformation. As shown in "Fig.4", the flexible wheel has less compaction resistance and hence larger values for the drawbar pull in comparison to the rigid wheel with the same dimension. Negative drawbar pull values means that the wheel is not able to generate any forward motion; hence a much improved performance is achieved by the flexible wheel as indicated by models developed in this paper and numerical results. "Table 1" shows the first contact angle for both the rigid and the flexible wheels on loose sand. The flexible wheels result in a smaller contact angle than the rigid wheel due to the deformation in low depth loose sand. As results the flexible wheel has less sinkage in comparison to the rigid wheel ("Table 2").

Table 1: First contact angle on loose sand

Rigid wheel first contact angle	Flexible wheel first contact angle
1.031 [Rad]	0.94 [Rad]

Table 2: Sinkage on loose sand

Rigid wheel sinkage	Flexible wheel sinkage
73 [mm]	61 [mm]

"Figure 5" shows that the flexible wheel acts as a rigid wheel on a sandy dune due to the small maximum pressure which terrain can support. In this case the performance of the model for flexible wheels developed in this paper produces very close values to the classical model for rigid wheels.

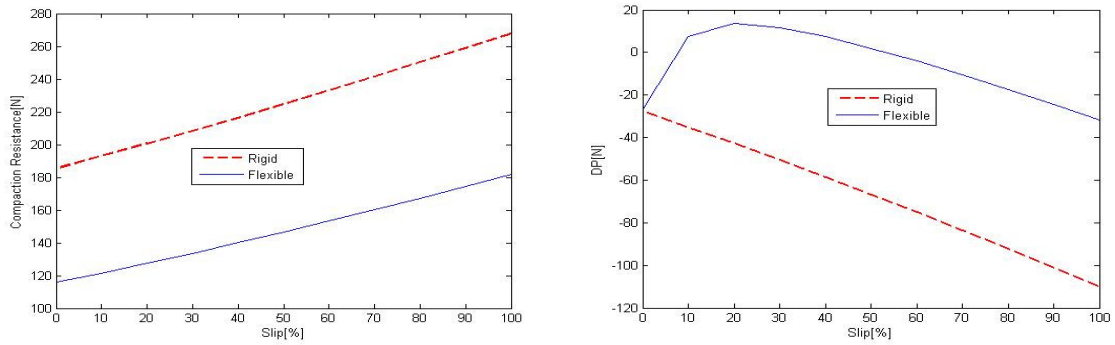

Fig. 4. DP and compaction resistance

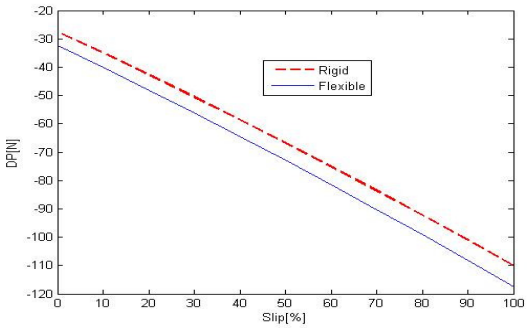

Fig. 5.Flexible wheel acts as rigid wheel

5. CONCLUSIONS

This paper presents a study for assessing the tractive capability of a flexible wheel operating in off-road conditions. Increasing the length of the contact patch between the wheel and the ground provides an increase in the tractive performance. The flexible wheel provides a larger contact patch due to the wheel's deformation under load. Analytical models are developed in this paper that predict the tractive performance for a flexible metal wheel by using the geometric model of the wheel in deformation. The analytical model is based on the ground pressure distribution over three contact sections with the ground. The proposed new analytical model illustrates that the flexible wheel can increase the length of the contact patch on soil surface. In turn, sinkage and compaction resistance are reduced and the traction force is increased. The developments have been validated by Finite Element Methods to show a close comparison with the analytical results. Simulation results presented in this paper illustrate that the flexible wheel increases the traction force in comparison to a rigid wheel with the same dimensions. Future work considering control systems for flexible wheels to maximize the traction force and minimize the slippage are under development.

6. REFERENCES:

[1] Bekker. M, "*Theory of land locomotion: the mechanics of vehicle mobility*" University of Michigan Press, Ann Arbor, USA, 1956.

[2] B. Lach, *"Individual tire inflation management for multi-axle vehicle"* IKK university der Bundeswehr Hamburg, 1999.

[3] Sreenivasan. S, and Wilcox. B, "Stability and traction control of an actively actuated micro rover". *Journal of Robotic system* 11(6):487-502, 1994.

[4] Dubowsky. S, Moore. C, and Sunada. C, "On the design and task planning of power-efficient field robotic systems" *Proceedings of the 6th ANS Robotics and Remote Systems Conference,* 1995.

[5] Farritor, S., Hacot, H., and Dubowsky, S.. "Physicsbased planning for planetary exploration". *Proceedings of the IEEE International Conference on Robotics and Automation (ICRA)*, Leuven, Belgium, pp. 278–283, 1998.

[6] Rover Team "*Pasteur Exobiology Payload and Rover For ExoMars: Technical Note 2/3 Design Concepts and trade-off Analysis*" EADS Astrium Ltd Technical Note ROV.TN2/3.01.EU.ASTR.C, Stevenage, UK, 2004.

[7] Bekker. M, "*Introduction to Terrain Vehicle System Part 1- The Terrain and Part 2- The Vehicle*" University of Michigan Press, Ann Arbor, USA, 1969.

[8] Wong. J, "*Theory of Ground Vehicles*" 2nd Edition, John Wiley &Sons, New York, USA, 2001.